

# Solar wind velocity dependence of the flow of galactic cosmic rays perpendicular to the ecliptic plane on the polarity of the interplanetary space magnetic field

**H. Kojima,<sup>a,\*</sup> S. Shibata,<sup>c</sup> H. Takamaru,<sup>b</sup> A. Oshima,<sup>b</sup> T. Koi,<sup>b</sup> K. Yamazaki,<sup>b</sup> T. Tabata,<sup>b</sup> S. Kawakami,<sup>d</sup> Y. Hayashi,<sup>d</sup> K. Tanaka,<sup>e</sup> T. Nakamura,<sup>f</sup> T. Nonaka,<sup>g</sup> S.K. Gupta,<sup>h</sup> P.K. Mohty,<sup>h</sup> K.P. Arunbabu,<sup>i</sup> M. Chakraborty,<sup>h</sup> S.R. Dugad,<sup>h</sup> B. Hariharan,<sup>h</sup> P. Jagadeesan,<sup>h</sup> A. Jain,<sup>h</sup> S. Mahapatra,<sup>h</sup> P.K. Nayak,<sup>h</sup> D. Pattanaik,<sup>h</sup> M. Rameez,<sup>h</sup> K. Ramesh,<sup>h</sup> L.V. Reddy,<sup>h</sup> P. Subramanian<sup>j</sup> and M. Zuberi<sup>h</sup>**

<sup>a</sup>*Chubu Astronomical Observatory, Kasugai-shi, Aichi 487-8501, Japan*

<sup>b</sup>*Faculty of Science and Engineering, Chubu University, Kasugai-shi, Aichi 487-8501, Japan*

<sup>c</sup>*Center for Muon Science and Technology, Chubu University, Kasugai-shi, Aichi 487-8501, Japan*

<sup>d</sup>*Graduate school of science, Osaka City University, Sugimoto-cho, Osaka 558-8585, Japan*

<sup>e</sup>*Hiroshima City University, Hiroshima 731-3166, Japan*

<sup>f</sup>*Faculty of Science, Kochi University, Kochi 870-8072, Japan*

<sup>g</sup>*Institute for Cosmic Ray Research, Tokyo University, Kashiwa, Chiba 277-8582, Japan*

<sup>h</sup>*Tata Institute of Fundamental Research, Homi Bhabha Road, Mumbai 400005, India*

<sup>i</sup>*St. Albert's College, Ernakulam 682018, India*

<sup>j</sup>*Indian Institute of Science Education and Research, Pune 411021, India*

*E-mail:* [hkojima@isc.chubu.ac.jp](mailto:hkojima@isc.chubu.ac.jp)

We have continuously observed muon intensities from 2000 to the present using the multi-directional muon telescope GRAPES-3 in Ooty, South India. The radial diffusion coefficient and the mean free path of propagation of the Galactic cosmic rays (GCR) in the heliosphere have been derived from the density gradient obtained from the flow perpendicular to the ecliptic plane of GCR, which depends on the polarity of the interplanetary magnetic field (IMF) (Kojima et al., 2018). In this study, we used the data set for the years 2000-2021, covering about 8,000 days and divided into 13 groups by the solar wind velocity to examine the relationship between the amplitude and phase of the flow as mentioned above of each group with the average solar wind velocity on the corresponding group. This analysis shows a positive correlation between the amplitude and phase of the flow of galactic cosmic rays perpendicular to the ecliptic plane, depending on the polarity of the IMF and the solar wind velocity.

38th International Cosmic Ray Conference (ICRC2023)

26 July - 3 August, 2023

Nagoya, Japan



\*Speaker

## 1. Introduction

Radial anisotropy of the galactic cosmic rays within inner heliosphere was theoretically studied by E.N.Parker and others within the framework of diffusion–convection model. It is known that the solar wind is responsible for sweeping out the galactic cosmic rays, creating a radial density gradient of cosmic rays that results in a tiny amount of anisotropy superposed on a larger isotropic component. The streaming of cosmic ray particles in the heliosphere could be composed of two components, one is the streaming in the ecliptic plane and the other one perpendicular to the ecliptic plane. The streaming in the ecliptic plane can be recorded by the ground based detectors as a diurnal variation in the counting rate, known as the Solar Diurnal Anisotropy. However, the streaming perpendicular to the ecliptic plane in the north–south direction is observed as a sidereal diurnal variation by the ground based detectors. This variation is caused by the streaming of cosmic rays produced by  $\mathbf{B} \times \mathbf{G}_r$  effect which is perpendicular to the ecliptic plane along the north–south direction [5][6]. Here  $\mathbf{B}$  is the IMF and  $\mathbf{G}_r$  is the radial density gradient of the galactic cosmic rays in the heliosphere. The main reason of this diurnal variation in sidereal time produced by the streaming of the cosmic rays along north–south direction is the tilted rotation axis of Earth relative to the ecliptic plane. A simple diffusion–convection equation without any time dependent terms as expressed by the following equation was used,  $V_{sw}n + \kappa \nabla n = 0$ , where,  $n$  and  $\nabla n$ , are the density and radial density gradient of cosmic rays,  $\kappa$  and  $V_{sw}$  represent the diffusion coefficient and the solar wind velocity. Here, the radial density gradient  $\mathbf{G}_r$  and  $n$  are related by  $\mathbf{G}_r = \nabla n/n$ . The diffusion coefficient may be used to obtain the value of the mean free path of propagation of the galactic cosmic rays in the heliosphere.

We have estimated the value of mean free path of the galactic cosmic rays at energy of 77 GV by using two independent methods. We have obtained the relations between variations of the cosmic ray intensity observed by the large area GRAPES-3 muon telescope ( $560 \text{ m}^2$ ) at Ooty (11.4 latitude, 76.7 longitude and 2,200 m altitude) in India and the variations of the solar wind velocity [3]. We also have obtained the radial density gradient of cosmic rays near Earth from the amplitudes of phase reversal of cosmic ray sidereal anisotropies on the polarity of the IMF [2]. From these quantities and the one dimensional diffusion convection equation that can explains the propagation of cosmic rays in the Heliosphere, we have derived the diffusion coefficient of the galactic cosmic rays in the IMF plasma [4]. Then, we have explained the role of the variation of the solar wind velocity on the propagation process of the cosmic rays in the Heliosphere. In this paper we examine the relationship between the amplitude and phase of the flow of galactic cosmic rays with the average solar wind speed.

## 2. Instrument

The galactic cosmic rays hitting the Earth's atmosphere can produce a number of secondary particles. However, among the secondary particles, neutrons and muons reach the ground level and can be utilized to study the near Earth space by the detectors placed on the ground. GRAPES-3 multi-directional muon telescope is consisted of 16 modules, which are detector units, each having 232 proportional counter tubes [1]. The proportional counter tube is made of steel and has dimensions  $10 \text{ cm} \times 10 \text{ cm} \times 600 \text{ cm}$ . Each detector module has 4 layers of 58 proportional

counter tubes. Each layer are placed in orthogonal direction along the proportional counter tube that enables us to measure arrival direction of atmospheric muon with an angular resolution of about  $10^\circ$ . Threshold energy for vertical muon is set to be around 1 GeV by absorber layers of 2.5 m thickness in total, which is made of concrete blocks. We are counting penetrating muon and categorizing into  $15 \times 15 = 169$  fine directions and  $3 \times 3 = 9$  coarse directions by using hit pattern marked by muon, each directions are labeled such as "V" for vertical. The large area of the detector  $560 \text{ m}^2$  enables us to perform high statistical observation. Figure.1 shows the schematic view of muon module. In this paper, we utilize only the data of "V".

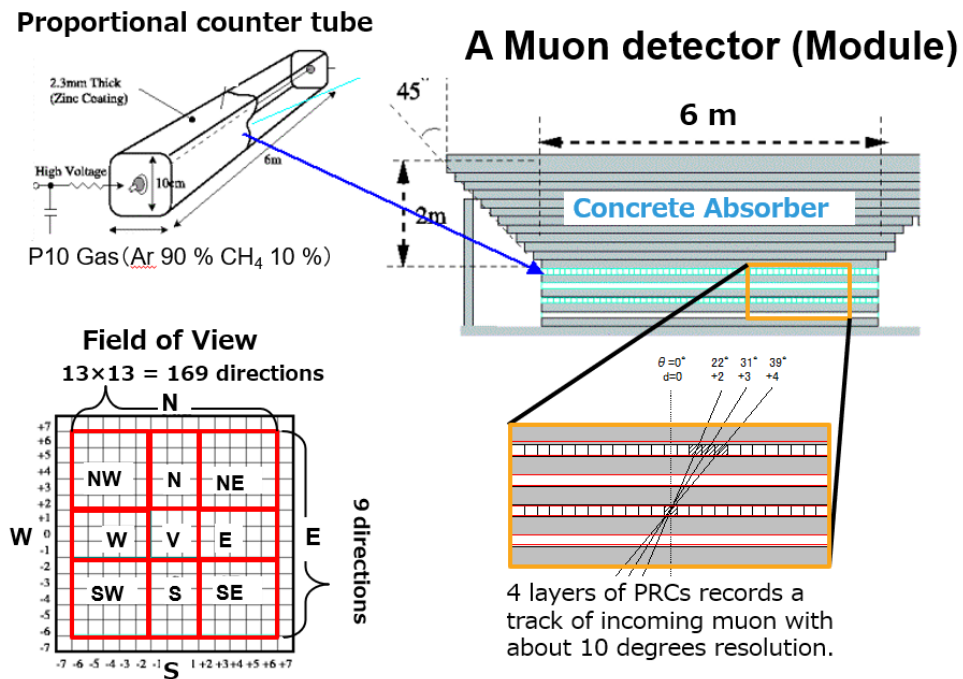


**Figure 1:** GRAPES-3 muon telescope consists of 16 muon tracking detectors which is called module.

### 3. Analysis

The GRAPES-3 muon telescope, composed of 16 modules each having four layers of proportional counter tubes, has an area of  $560 \text{ m}^2$  and records the counting rate of muons at approximately 10-second intervals. The data obtained by the GRAPES-3 muon telescope are divided into nine directional components, as mentioned in the previous section, as the original data in this analysis. We have conducted an analysis for daily variation of cosmic rays according to the following procedure. We must remove abnormal values from the original data for each modules. At first, we aggregate the data from 10-second values to 1-hour values year by year and obtain a set of 22 years hourly data. Then we calculate the annual average value and standard deviation ( $\sigma$ ) of the 1-hour values. If any hourly values deviate more than  $10\sigma$  from the average values, the data is marked as an abnormal value and set to be lack of data and removed from the analysis. After this removal of abnormal data by  $10\sigma$  criteria, the annual average value and standard deviation ( $\sigma$ ) are calculated once again. If

any hourly values deviate more than  $5\sigma$  from the average value are removed as the same way as  $10\sigma$ . For these new data set, we calculate percentage hourly values of variation throughout a year. For these percentage hourly values, atmospheric pressure correction is performed (for V component,  $-0.12\%/\text{(hPa)}$  has been used). After the atmospheric pressure correction, a 647-hour (27 days) moving average is calculated and subtracted from the percentage hourly data, which is equivalent to perform a high-pass filter. The data, further processed through a 24-hour high-pass filter, is the foundational data for daily variation analysis.

The data of vertical direction of GRAPES-3 muon telescope contains approximately 8,000 days over 22 years. A daily variation were determined as values for each sidereal time based on the hourly observational values. For the data of these 8,000 days, the data was divided into 13 groups based on the magnitude of the daily mean value of the solar wind, 300 km/s, 326 km/s, 339 km/s, 359 km/s, 374 km/s, 390 km/s, 406 km/s, 426 km/s, 450 km/s, 478 km/s, 515 km/s, 569 km/s, 656 km/s. We adopted the solar wind data "Plasma (Flow) speed km/s daily average" from the Omni2 data [7]. For each groups, containing about 600 days, the data was divided into IMF polarity "Toward" and "Away" and was calculated sidereal time variation for each day. In our analysis, the "Toward" and "Away" are decided as the following way. At first, the 72-hour moving average are performed for the Omni2 IMF  $B_x$  and  $B_y$  values. If a day where the  $B_x$  value was negative and the  $B_y$  value was positive for through out the day (24 hours), the day were decided to be "Toward", while a day with positive  $B_x$  and negative  $B_y$ , were 'Away'. In this paper, we denote "Toward" as "T" and "Away" as "A" for each sidereal time variation. After calculation of sidereal daily variation for Toward and Away, the  $(T-A)/2$  was calculated, and its amplitude and phase were determined. The above mentioned process was applied for each of the 13 groups of the solar wind velocity to detect their amplitude and phase (Figure.2, Figure.3, Figure.4, Figure.5, Figure.6). Here the amplitude was calculated by dividing the difference between the maximum and minimum of sidereal daily variation by two, while the phase was determined as the maximum of the sidereal daily variation.

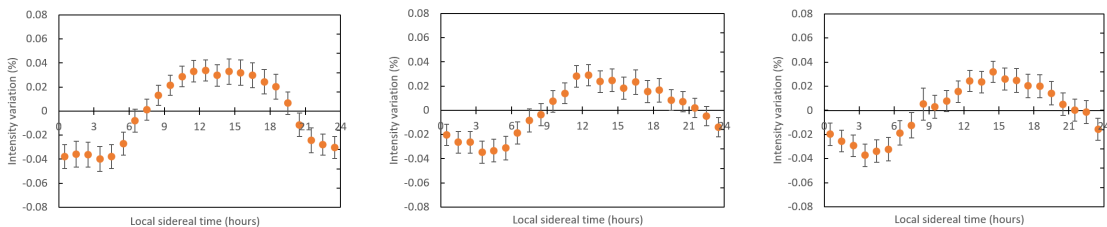


**Figure 2:** Cosmic ray intensity variation in local sidereal time categorized into the solar wind velocity of 300 km/s, 326 km/s, 339 km/s

## 4. Results

The amplitude and phase of the  $(T-A)/2$  sidereal daily variation for each group of the solar wind velocity were plotted against the average solar wind velocity (Figure.7, Figure.8). The average solar wind velocity for each group was calculated by the simple average of the solar wind velocities for each day. The  $(T-A)/2$  sidereal daily variation amplitude, which represents the magnitude of the sidereal anisotropy (Swinson flow) originating from the cosmic ray flow in the direction

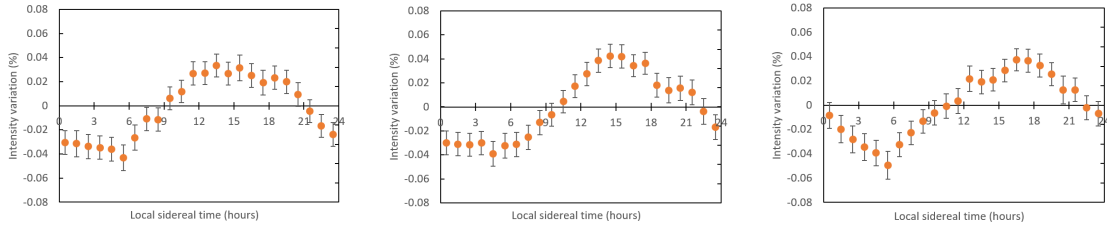


**Figure 3:** Cosmic ray intensity variation in local sidereal time categorized into the solar wind velocity of 359 km/s, 374 km/s, 390 km/s

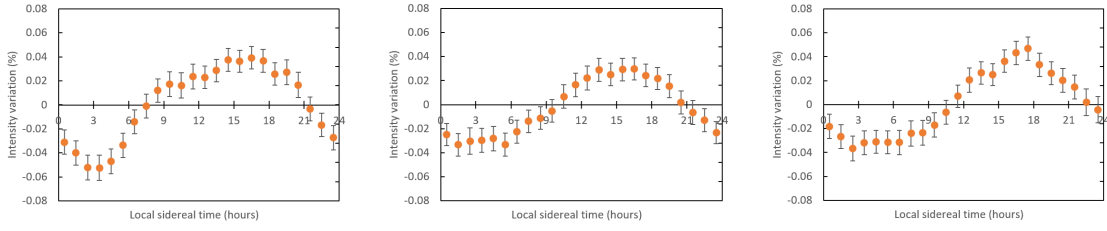


**Figure 4:** Cosmic ray intensity variation in local sidereal time categorized into the solar wind velocity of 406 km/s, 426 km/s, 450 km/s

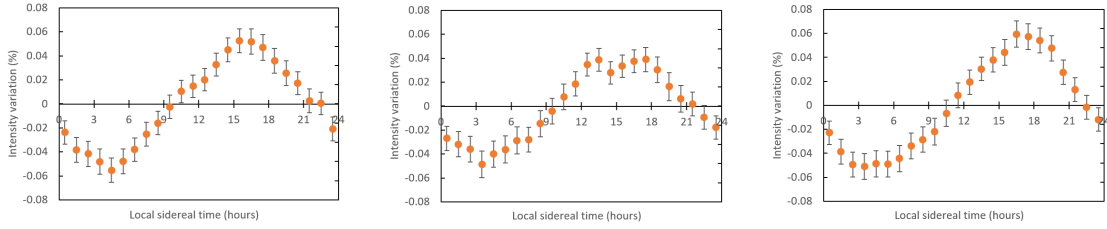


**Figure 5:** Cosmic ray intensity variation in local sidereal time categorized into the solar wind velocity of 478 km/s, 515 km/s, 569 km/s

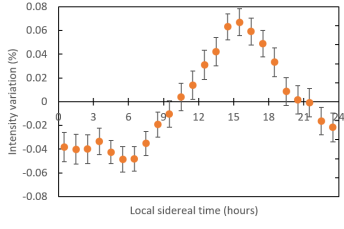


**Figure 6:** Cosmic ray intensity variation in local sidereal time for the solar wind velocity of 656 km/s

perpendicular to the ecliptic plane. Figure 7 shows a clear correlation with solar wind velocity. On the other hand, the phase keeps constant even when the solar wind velocity changes (Figure 8). This also shows a characteristics the Swinson flow.

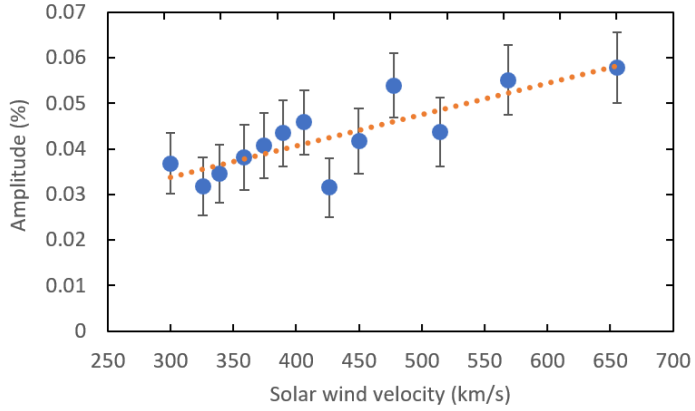


**Figure 7:** Dependency of the amplitude of cosmic ray variation in local sidereal time on the solar wind velocity.

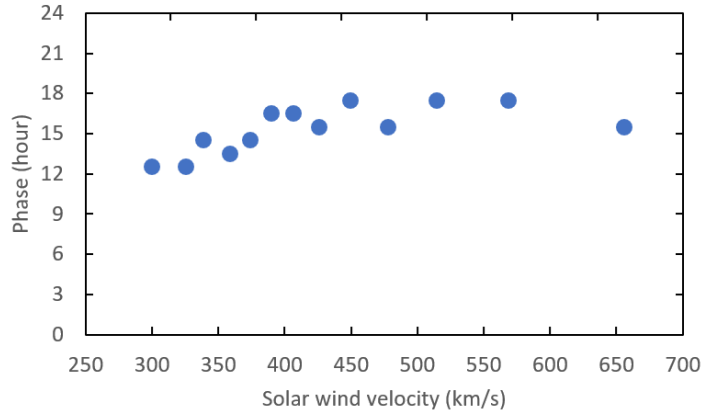


**Figure 8:** Dependency of the phase of cosmic ray variation in local sidereal time on the solar wind velocity.

## 5. Acknowledgement

The authors would like to thank all the staff of the GRAPES-3 experiment at Cosmic Ray Laboratory in Ooty and Tata Institute of Fundamental Research in Mumbai for their effort to operation of the experiment. This work is partially supported by the joint research program of the Institute for Space-Earth Environmental Research (ISEE), the Nagoya University. We should thank to the omni group for their effort to maintain the OMNI data at the GSFC/SPDF OMNIWeb [8] which was important for this analysis.

## References

[1] Y.Hayashi et al.: A large area muon tracking detector for ultra-high energy cosmic ray astrophysics - the GRAPES-3 experiment. Nucl. Instrum. Methods A 545, 643 (2005)

[2] H. Kojima et al., Measurement of the radial density gradient of cosmic ray in the heliosphere by the GRAPES-3 experiment , Astropart. Phys. 62 (2015) 21.

[3] H. Kojima et al., Dependence of cosmic ray intensity on variation of solar wind velocity measured by the GRAPES-3 experiment for space weather studies , Phys. Rev. D 91 (2015) 121303(R).

[4] H. Kojima et al., Measurement of the radial diffusion coefficient of galactic cosmic rays near the Earth by the GRAPES-3 experiment, Phys. Rev. D 98, 022004 (2018)

[5] D. B. Swinson, ‘Sidereal’ Cosmic-Ray Diurnal Variations , J. Geophys. Res. 74 (1969) 5591.  
D. B. Swinson, Field Dependent Cosmic Ray Streaming at High Rigidities , J. Geophys. Res. 81 (1976) 2075.

[6] S. Yasue, North-South Anisotropy and Radial Density Gradient of Galactic Cosmic Rays , J. Geomag. Geoeletr. 32 (1980) 617.

[7] OMNI 2 Preparation. <http://omniweb.gsfc.nasa.gov/html/omni2doc.html>